MEASUREMENT OF THE SURFACE ENERGY OF RAW AND LUBRICATED LACTOSE POWDERS BY INVERSE GAS CHROMATOGRAPHY

By

JITENG XU

A thesis submitted to the

Graduate School of Studies

Rutgers, The State University of New Jersey

In partial fulfillment of the requirement

For the degree of

Master of Science

Graduate Program in Chemical and Biochemical Engineering

And approved by

_____

_____

_____

New Brunswick, New Jersey

May, 2019

ABSTRACT OF THE THESIS

Measurement of the surface energy of raw and lubricated lactose by inverse gas chromatography

By JITENG XU

Thesis Director:

Gerardo Callegari and German Drazer

Engineers and pharmacists have shown that in particle processing operations such as milling, granulation, crystallization and powder mixing, the surface energy of the starting, intermediate or final products is a key factor to understand the outcome of the operation and the final product performance. Since its establishment in the 1940s, inverse gas chromatography (IGC) is a powerful, sensitive and relatively fast technique for characterizing the surface properties of pharmaceutical powders. The feasibility of using IGC to investigate changes in surface energy of pharmaceutical powders depending on particle size of the powder and on the magnitude of shear strain applied to a pharmaceutical blend is considered in this thesis. Two powder materials, an excipient and a lubricant, are used. The excipient is lactose monohydrate powder sieved to obtain particles in the following size ranges: 38-45, 45-53, 53-63, 63-75, 75-90, and 90-106μm. The lubricant is magnesium stearate (MgSt). The blends were mixed using a V-blender and a controlled amount of mechanical shear strain was applied to the blend by using an ad-hoc modified Couette shear cell. It was found that the surface energy of lactose has no significant

dependence on particle size. We also show that there is a measurable reduction in the dispersive energy of lactose-MgSt blends.

Acknowledgement

I would first like to thank my thesis advisors, Dr. Gerardo Callegari and Dr. German Drazer, for giving me the opportunity to work on this project and encourage me to devote my thesis on it. Their inspiring advices, patient instructions and immense support guided me throughout my research. I would also like to thank the Engineering Research Center for Structured Organic Particulate Systems (ERC-SOPS) for providing all the resources and facilities needed in my research.

Contents

List of tables

List of Figures

1.Introduction

The discovery of chromatography was made by the American petroleum chemist David T. Day and the Russian botanist Mikhail S. Tswett between 1903 and 1906 [1]. In the original experiments by Tswett, plant pigments were separated into colored bands as they eluted through a bed of powdered calcium carbonate. Tswett was the first to recognize the sequential sorption-desorption interaction of chromatographic processes. After the pioneering work of Tswett, other forms of chromatography were developed, such as gas chromatography (GC). In GC a column is used to separate and characterize gases and vapors. In a very short time, gas chromatography become an important method for separation and analysis of compounds. Then in 1940, inverse gas chromatography (IGC), a new type of gas chromatography was first introduced by Martin and Synge. Compared to GC, the term "inverse" indicates that the sample to be examined is placed in the chromatography column and probe molecules are injected into it [1]. Inverse gas chromatography has become a powerful technique for determining the surface and bulk properties of substances in many areas, including food industry [3], polymer materials [4] and pharmaceutical industry[2]. IGC is considered a material characterization method, providing information about properties such as surface energy heterogeneity, surface acid-base properties, glass transition, adsorption isotherm, solubility parameters, BET surface area, work of cohesion and work of adhesion. The most frequent use of IGC in the last decade is for the study of the surface properties of powders [3]. Surface properties are dely described in term of the surface free energy, commonly referred-to simply as the 'surface energy' of the material.

Knowledge of surface properties is important in the formulation and manufacture of modern pharmaceutical particulate products. In fact, during the past decade and more,

particle engineers and pharmacists have worked to understand and control a range of key unit manufacturing operations such as milling, granulation, crystallization, powder mixing and dry powder inhaled drugs. It has become increasingly clear that, in many of these particle processing operations, the surface energy of the starting, intermediate or final products can be a key factor in understanding the processing operation and the performance of the final product [4]. Several methods exist for measuring the surface energy for pharmaceutical powders [4]. However, many of them have important limitations. IGC has several advantages over other techniques for the analysis of the surface properties of pharmaceutical powders, such as the ability to analyze the powder without pre-treatment, a high level of reproducibility, a simple experimental setup, and rapid data collection [5].

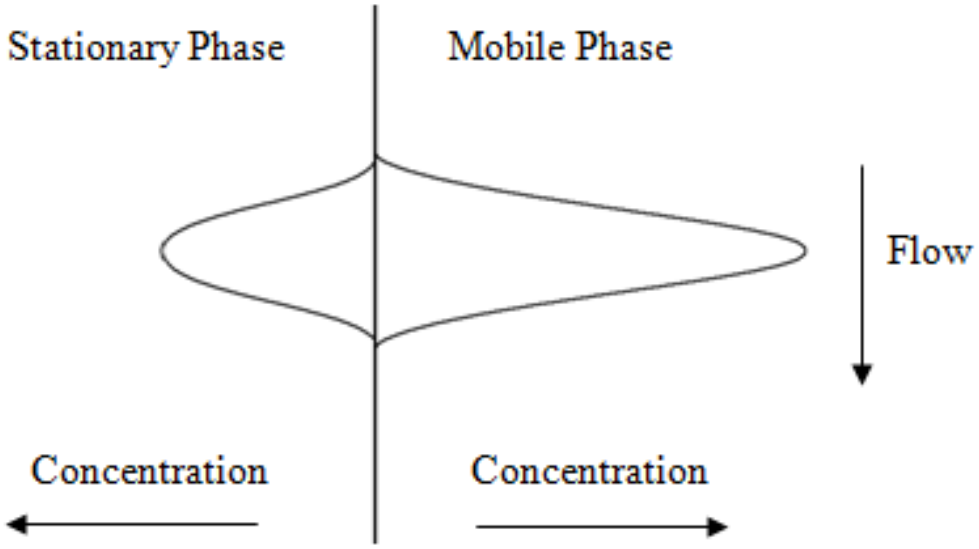

Fig.1 Representation of the concentration profiles for a compound distributed between the stationary (left) and mobile (right) phases of a chromatographic column.

The principle of inverse gas chromatography is essentially the opposite of conventional gas chromatography. In IGC an empty glass column is uniformly packed with a solid sample

of interest, typically a powder, fiber or film. Then, to analyze the stationary phase, a low concentration of a well-characterized single gas or vapor (the *probe* or *probe molecule*) of a volatile substance is injected through the column and carried by an inert gas at a fixed flow rate [6]. The most commonly used carrier gases are helium, argon, and nitrogen [6]. After the compound of carrier gas and probe is injected into the column, it will distribute into the mobile and the stationary phases in the column. Fig.1 represents the concentration distribution profiles in the two phases. We can see for this compound that the concentration distribution in the mobile phase is bigger, which means it typically travel down the column faster than a compound that has more distribution in the stationary phase.

The distribution of stationary and mobile phases can be described by the partition coefficient (unit: unit length), K_R, which is related to the concentration of adsorbate in the mobile phase (unit: mass/mole per unit area), c_M, and that in the stationary phase (unit: mass/mole per unit volume), c_s, via:

$$K_R = \frac{c_S}{c_M} = \frac{V_N}{\sigma m_s} \tag{1}$$

The partition coefficient is also directly related to the mass of the solid, m_s, the specific surface area of the solid, σ, and the net retention volume, V_N, which is defined as the volume of carrier gas required to elute the injected adsorbate through the column. Both K_R and V_N depend on the strength of the interaction between the adsorbate and the stationary phase.

Eventually, the compound will leave the column and pass through a detector, and the output signal of the detector creates what is called a chromatogram.

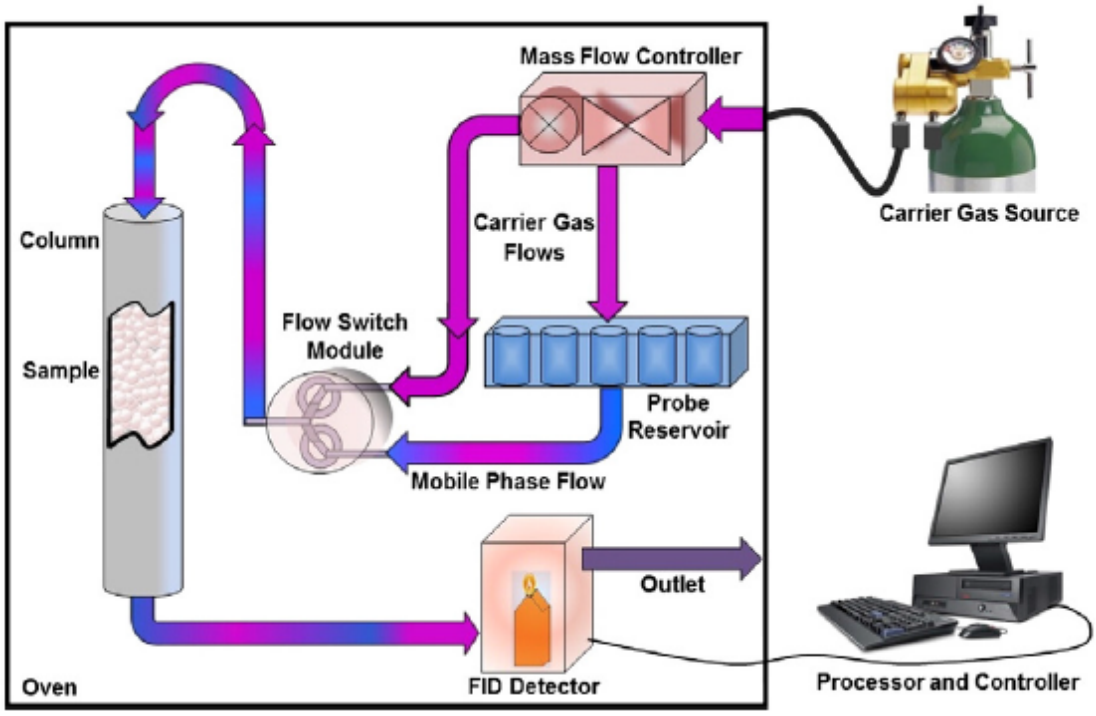

Fig.2 schematic illustration a typical inverse gas chromatography analyser

The IGC apparatus contains a control PC, a flow control module, a probe gas oven, and a sample column oven. Ten different vapor probes and the vapor humidifier are all kept in the probe gas oven at a specified temperature in order to maintain accuracy and ensure repeatability of injections. The sample column oven allows the sample to be examined at different temperatures. The two detectors typically used in gas chromatography are the thermal conductivity detector (TCD) and the flame ionization detector (FID) [6]. The flame ionization detector is more frequently used because it is more sensitive to all compounds containing C-C and C-H bonds. It measures the change in electric conductivity of a hydrogen flame in an electric field when in the presence of organic compounds [6]. The schematic illustration of a typical IGC apparatus is shown in Fig.2.

By controlling the amount of probes injected into the column two chromatographic conditions, finite dilution and infinite dilution, and experiments can be performed under both conditions in the IGC apparatus [7].The Infinite dilution condition is obtained by injecting a very small amount of probe molecules into the system (typically <3% of the partial pressure of the probe). Infinite dilution is commonly used to evaluate the surface energy and heat of sorption of the solid [8]. Since the amount of probe molecules (or adsorbate) is small, it results in a very small surface coverage on the adsorbent. Therefore, the adsorption at infinite dilution is also called 'adsorption at zero surface coverage' [9]. Adsorption under the infinite dilution condition follows Henry's Law[10]. Because of the amount of probe molecules adsorbed is linearly dependent on the injection concentration, chromatographic peaks under the infinite condition are typically symmetrical and Gaussian in shape. The measured data in this method is net retention time and it is the key parameter to determine the dispersive component of surface free energy, acid-base properties of the surface, surface polarity, activity coefficients, Flory-Huggins, thermodynamic interaction, free energy of adsorption and surface heterogeneity, surface activity and adsorption entropy [7].When the injection concentration of the experiment is increased beyond the range of validity of Henry's Law, the experiment is then referred to as in the finite concentration regime [11]. Our measurements are all under the infinite dilution condition. In our experiments, the second generation of IGC surface energy analyzer (Surface Measurement System Ltd. (SMS), London, U.K.) was used. Because in infinite condition the amount of probe molecule or adsorbate is limited, it is assumed that interactions first occur only with the high-energy sites on the surface and therefore interactions with the lower energy sites are negligible at low coverages. By increasing the surface coverages,

more high energy sites will be covered and finally lower energy sites will also be covered. Then we will have the average surface energy of the solid surface and the distribution of surface energy at different surface coverages. The theory of surface energy calculation is introduced in the next section.

The feasibility of using IGC to investigate changes in surface energy of pharmaceutical powders depending on particle size of the powder and on the magnitude of shear strain applied to a pharmaceutical blend is considered in this study. The specific goals of our study were to determine: (i) if there is a change in the surface energy with a different particle size of lactose, (ii) if there is a change in the surface energy of lactose following lubrication with MgSt when the blend is subjected to different processing conditions (shear strain).

2. Theory of surface energy measurement by Inverse Gas Chromatography (IGC)

One of the most widely used and interesting applications of the IGC is the measurement of surface free energy. The retention time and retention volume are the fundamental parameters that can be obtained from the method, which can generate a peak as a result of interactions between the probe molecule and the stationary phase. The total surface energy is the sum of the dispersive and the specific components. The first one takes into account non polar molecular interactions, while the second includes polar interactions like the ones produced between acid and base groups, the most common of this kind of interaction is the Hydrogen-bond.

2.1 Dispersive component of surface energy

There are two methods that can be used to calculate the dispersive surface energy component of a solid through IGC: Schultz[12] and Dorris-Gray[13]. Here, we chose to use Schultz method as both are generally giving very similar results and the Schultz method is more commonly used [12, 14]. The calculation is based on the retention parameter of liquid n-alkane probes at infinite dilution. Alkanes are used because they do not interact through acid-base interaction[15]. The retention time is proportional to the strength of molecular interactions between the probe and the solid surface of sample packed in the column. The dead time, t_0, is the time required to elute an un-retained solute to pass through the column, as the gas methane is usually not retained in any solid material, it is usually

used to measure the dead time of. After the dead time is obtained, the net retention time of any probe is calculated as the time it takes for that probe to pass through the sample minus the dead time (or the time it takes methane to elute). Hence, net retention volume of the probe can be expressed as[16]:

$$V_N = j\, F_c(t_R - t_0) \tag{2}$$

Where F_c is the carrier gas flow rate in the column and j is the James-Martin correction factor which corrects the net retention time for the pressure drop inside the column and variation in packing density of the solids within the column bed. The James-Martin correction factor, j, is defined as[9]:

$$j = \frac{3}{2}\left[\frac{(P_{in}/P_{out})^2 - 1}{(P_{in}/P_{out})^3 - 1}\right] \tag{3}$$

Where P_{in} and P_{out} are the inlet and outlet pressure.

In order to eliminate the effect of temperature and the quantity of the stationary phase, specific retention time is used instead of the net retention time. Specific retention volume is expressed as[16]:

$$V_g^0 = \left(\frac{v_N}{m_s}\right)\left(\frac{273.15}{T}\right) \tag{4}$$

Where is the specific retention volume at 0 ℃and m_s is the mass of the sample. Therefore, by combining Eqs. (2) and (4), the specific retention volume can be expressed as[16]:

$$V_g^0 = \left(\frac{j}{m_s}\right) F_c\,(t_R\text{-}t_0)\,\left(\frac{273.15}{T}\right) \quad (5)$$

Interactions between an adsorbate and absorbent are either dispersive or specific as described above. Dispersive and specific components of surface Gibbs energy are calculated from thermodynamic equations. The standard Gibbs free energy change is related to the net retention volume, V_N, as follows[16, 17]:

$$\Delta G_{ad}^0 = \Delta G_{de}^0 = RT\ \ln V_N + C \quad (6)$$

Δ is the standard molar Gibbs free energy changes of absorption and Δ is the standard molar Gibbs free energy changes of desorption. R and T are the gas constant and absolute temperature (K) and the constant C is indicative of the reference states. The free energy of adsorption (ΔG_{ad}^0) is the sum of the dispersive (ΔG_{ad}^D) and specific (acid-base, ΔG_{ad}^{SP}) components of the free energy of adsorption [18]:

$$\Delta G_{ad}^0 = \Delta G_{ad}^D + \Delta G_{ad}^{SP} \quad (7)$$

The assumption is that these two contributions are additive. When n-alkanes are used as probes, there are no specific interactions with the stationary phase. Therefore $\Delta G_{ad}^0 = \Delta G_{ad}^D$ and their value depends on the number of carbon atoms in the alkane molecule[16, 19] . The free energy of adsorption can be expressed as:

$$-\Delta G_{ad}^{0} = N_A\, a\, W_{adh} \quad (8)$$

Where N_A is Avogadro's number (mol^{-1}), a is the cross-sectional area of the probe molecule (m^2), and W_{adh} is the work of adhesion (mJ m^{-2}), which is related to the dispersive free energy of solid and liquid interaction by Fowke's equation[20]:

$$W_{adh} = 2\sqrt{\gamma_S^D \gamma_L^D} \quad (9)$$

Where γ_S^D and γ_L^D are the dispersive components of the surface free energy of the solid and the dispersive components of the surface free energy of probe molecule. Combining Eqs. (6), (8), and (9) yields the following equation[11, 12, 14]:

$$RT\ \ln V_N = 2N_A\, a \sqrt{\gamma_S^D \gamma_L^D} + C \quad (10)$$

Thus, a plot of $RT\ln V_N$ versus $a\sqrt{\gamma_L^D}$ for a homologous series of n-alkanes is linear, it is known as the "alkane line". The dispersive surface energy (γ_S^D) of the stationary phase can be calculated from the slope of the linear regression the n-alkanes line. Unlike the n-alkanes points, polar probes do not lie on the alkane line. The vertical distance between the alkane line and the polar probes is the specific component of the Gibbs free energy[9].

2.2 Specific component of surface energy

To determine the specific or non-dispersive components, also termed the acid-base interaction parameters of surface free energy, γ_S^{sp}, the dispersive component is subtracted from the total free energy of adsorption . Van Oss, Chaduary and Good approach is used to determine the acid-base interaction of surface free energy, γ_S^{sp}. This approach is based on the interaction between each of two monopolar probes (one acidic and one basic probe – e.g. ethyl acetate ($C_4H_8O_2$) and dichloromethane (CH_2Cl_2) [21]) with the solid surface. ΔG^{sp} follows the equation[22]:

$$-\Delta G = 2N_A a\left(\sqrt{\gamma_s^+}\gamma_l^- + \sqrt{\gamma_s^-}\gamma_l^+\right) \tag{11}$$

The base parameter (γ_S^+) is calculated from the specific component of the free Gibbs energy between the acid monopolar vapor (ethyl-acetate) and the solid. In a similar way, the acid parameter (γ_S^-) of the solid surface is calculated from the specific component of the free Gibbs energy between the base monopolar vapor (dichloromethane) and the solid surface. The total specific component of the solid surface energy can be calculated as that we used in our experiments, respectively [22]:

$$\gamma_S^{SP} = 2\sqrt{\gamma_S^+\gamma_S^-} \tag{12}$$

In vOGC scale, the $\gamma_l^+ \; and \; \gamma_l^-$ of dichloromethane are 5.2 mJ/m^2 and 0 mJ/m^2, the $\gamma_l^+ \; and \; \gamma_l^-$ of ethyl acetate are 0 mJ/m^2 and 19.2 mJ/m^2.

2.3 Adsorption isotherm

The adsorption isotherm is the relation between the amount of gas adsorbed and the equilibrium pressure of the adsorbates at a constant temperature. The partial pressures can be calculated with the following equation[3]:

$$p = \frac{n_i R H_{peak} 273.15}{F \cdot A_{peak}} \tag{13}$$

where n_i is the moles of probe injected, R is the universal gas constant, H_{peak} is the FID signal, F is the carrier gas flowrate and A_{peak} is the area of the peak. Then, the adsorbed amounts normalized by the mass of the partial pressures of adsorbed were obtained by calculating the integral of specific retention volumes over the partial pressures of the adsorbate by the following equation [3]:

$$n = \frac{1}{RT} \int_0^p V_N dp \tag{14}$$

2.4 BET surface area determination

Brunauer–Emmett–Teller (BET) theory aims to explain the physical adsorption of gas molecules on a solid surface and serves as the basis for an important analysis technique for the measurement of the specific surface area of materials. BET method was developed in 1938 and over the years it has become one of the most common methods used for characterization of catalysts, adsorbent, and other artificial and natural porous materials[23, 24]. Surface area measurement is commonly based on the determination of an adsorption isotherm of a non-polar probe molecule[25]. The BET theory was developed with nitrogen

adsorption at 77 K and it has been established as a standard. To run a BET experiment with IGC organic solvents need to be used, the most common are octane, heptane, and cyclohexane. With the preference for octane, on the one hand, the probe molecule needs to be as small as possible to be able to adsorbed in any small roughness at the molecule level. On the other hand, the retention time cannot be too small to get a good volume retention resolution. Six types of isotherms can occur depending on the adsorption scenario[26]. The BET equation is only applicable to isotherms type II and IV and in these two types isotherm, there is a formation of a monolayer followed by multi-layers and further capillary condensation[27]. The BET equation is the following[28]:

$$\frac{1}{n[(P_0/P)-1]} = \frac{c-1}{n_m c}\left(\frac{p}{p_0}\right) + \frac{1}{n_m c} \tag{15}$$

Where P is the solvent partial pressure in the gas phase (Torr), P_0 is the saturated solvent vapor pressure (Torr), n is the amount of gas adsorbed (Mol g^{-1}), n_m is the monolayer capacity (Mol g^{-1}) . This equation is an adsorption isotherm and a straight line is taken by plotting the $1/n(P_0/P) - 1]$versus P_0/P [27]. The BET equation fits the isotherm type II or type IV with a specific range of equilibrium pressure P_0/P, usually for $0.05 < P_0/P < 0.35$. And the best points have to be selected in this range (where the R^2>0.995)[16]. It is important in case of the BET specific surface area determination that the injected solvent has to form the Type II or IV of isotherms, the Fig.3 shows the possible isotherm forms[29].

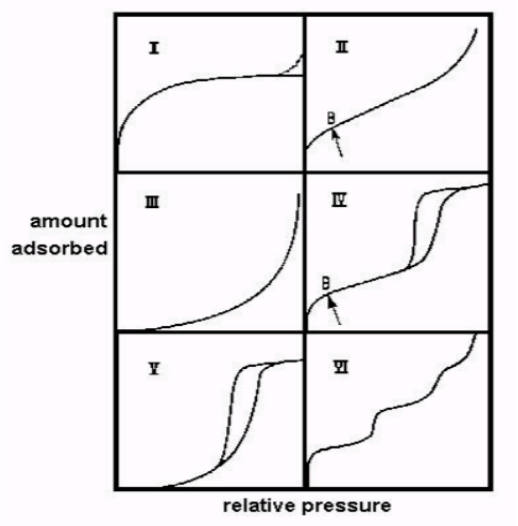

Fig.3: Six types of isotherms

The sorption constant (c) and the monolayer capacity (n_m) are calculated from the slope and intercept of the line. The surface area is determined by the following equation[27]:

$$S_{BET} = \frac{(n_m N_{Av} a)}{V \cdot m} \tag{16}$$

where n_m is the monolayer adsorbed gas amount, N_{Av} is the Avogadro's number, a is the adsorption cross section of the adsorbing species, V is the molar volume of adsorbed gas and m is the mass of adsorbent (g).

3. Materials and Methods

As mentioned before, all the experiments discussed in this thesis were performed with a fully automated IGC system (Surface Measurement System Ltd. (SMS), London, U.K.). Gas Chromatography grade decane, nonane, octane, heptane, hexane, dichloromethane, and ethyl acetate were used in our experiments. Each powder sample was packed into a silanized glass column (300mm 4mm i.d.) by tapping, until no cracks, hollows, or channels were visible in the powder bed. It is not necessary to fill the entire column but need a reasonable amount of surface to measure the retention time. Typically, by adding 1800mg lactose, we can obtain 0.3-0.5m/g specific surface area of lactose, which is typically sufficient to obtain bulk properties. The columns were loosely stoppered with silanized glass wool in both ends. Calculations were performed using SMS IGC Analysis software v1.3. Experiments method was set up by the software named Cirrus SEA.

Powder systems

Two different powder systems were studied. The first one was 100% Lactose powder with different particle sizes, 38-45, 45-53, 53-63, 63-75, 75-90, and 90-106μm. α-Lactose monohydrate (Foremost Farms USA) was used. The particle size distribution of the raw material in the drum is characterized by d50 value equal to 60um. Particle size distribution was measured using a Laser Diffraction Spectroscopy technique (Beckman-Coulter LS 13 320 series laser diffraction particle size analyzer). Material was collected from meshes: 90, 75, 63, 53, 45 and 38 μm. All samples were measured for three different surface coverages

2, 5, and 8%. One column of each sample was prepared. A measurement with a flow rate of 10 sccm (standard cubic centimeter per minute) was made on each of the columns. In some cases, an additional measurement with a lower flow rate of 5sccm was also performed. (In Table 1 in the next chapter we will present a table summarizing all the experiments performed as part of this thesis).

The second powder system, was a blend of 99% lactose using α-Lactose monohydrate (Foremost Farms USA) and adding 1% by weight of Magnesium Stearate (MgSt). Lactose and MgSt are widely used excipient and lubricant, respectively, in pharmaceutical formulations. The blend was then exposed to two different processing conditions. In both cases, 600g lactose and 6g MgSt powder were mixed in a V-blender for 3 minutes [30]. Then, we took out 300g and exposed them to a controlled amount of mechanical shear strain by a Couette shear cell. The Couette shear cell is designed to apply uniform flow and shear environment to the powder sample[31]. The blend was sheared for 32 minutes with a shear rate of 80 revolutions per minute, corresponding to 2560 revolutions in total. We shall refer to the sample that is only mixed in the V-blender as the *reference* sample and the one that is sheared in the Couette cell as the *sheared* sample. Both samples are packed in a silanized glass column of 30cm length and 4mm inner diameter. (The *reference* and *sheared* samples are columns 13 and 14, respectively, in Table.1.)

4. Results and discussion

We begin this chapter by presenting a list of all the experiments performed in this thesis in Table 1 below, including information on materials used and the retention time at 5% surface coverage for comparison.

Table.1: Experimental summary

materials information								Retention at 5% surface coverage						
Experiments	Column	Material	Component	Mass	Coverages	Flow rate	SSA	Decane	Nonane	Octane	Heptane	Hexane	Dichloromethane	Ethyl acetate
1	1	Lactose	100% Lactose 38-45mm	1736	2%, 5%, 8%	5	0.4036	12.121	4.512	1.401	0.515	0.164	0.069	0.492
2	1	Lactose	100% Lactose 38-45mm	1736	2%, 5%, 8%	10	0.4036	6.381	2.121	0.726	0.254	0.085	0.035	0.251
3	1	Lactose	100% Lactose 38-45mm	1736	5%	10	0.4036						0.035	0.251
4	1	Lactose	100% Lactose 38-45mm	1736	5%	10	0.4036						0.035	0.251
5	1	Lactose	100% Lactose 38-45mm	1736	5%	10	0.4036						0.035	0.251
6	2	Lactose	100% Lactose 38-45mm	1471	5%	10	0.4402						0.038	0.352
7	2	Lactose	100% Lactose 38-45mm	1471	2%, 5%, 8%	10	0.4402	7.352	2.36	0.838	0.274	0.088	0.038	0.352
8	3	Lactose	100% Lactose 45-53mm	1948	2%, 5%, 8%	10	0.288	4.146	1.509	0.534	0.186	0.054	0.022	0.157
9	3	Lactose	100% Lactose 45-53mm	1948	2%, 5%, 8%	10	0.3881	4.146	1.509	0.534	0.186	0.054	0.022	0.157
10	4	Lactose	100% Lactose 53-63mm	1667	2%, 5%, 8%	10	0.2566	4.555	1.582	0.541	0.183	0.058	0.02	0.156
11	5	Lactose	100% Lactose 53-63mm	1864	2%, 5%, 8%	10	0.3056	4.139	1.41	0.502	0.173	0..048	0.02	0.143
12	5	Lactose	100% Lactose 53-63mm	1864	2%, 5%, 8%	10	0.3056	4.139	1.41	0.502	0.173	0..048	0.02	0.143
13	6	Lactose	100% Lactose 53-63mm	1652	2%, 5%, 8%	10	0.3084	4.573	1.512	0.527	0.184	0.056	0.022	0.227
14	6	Lactose	100% Lactose 53-63mm	1652	5%	10	0.3084						0.022	0.227
15	7	Lactose	100% Lactose 63-75mm	2217	2%, 5%, 8%	5	0.2193	8.838	2.949	1.014	0.336	0.095	0.036	0.424
16	7	Lactose	100% Lactose 63-75mm	2217	2%, 5%, 8%	10	0.2193	4.642	1.51	0.59	0.175	0.049	0.029	0.194
17	7	Lactose	100% Lactose 75-90mm	2157	2%, 5%, 8%	10	0.159	3.022	1.028	0.398	0.13	0.038	0.015	0.128
18	8	Lactose	100% Lactose 90-106mm	2087	2%, 5%, 8%	10	0.1249	2.52	0.862	0.209	0.1	0.022	0.007	0.097
19	9	Carbopol	100% Carbopol	643										
20	10	Blend 0 rev(Vblend&Couette)	91% Lactose, 9% APAP, 1%MgSt	1744	2%, 5%, 8%	10	0.5021	15.365	5.083	1.736	0.597	0.205	0.093	0.883
21	11	Blend 640 rev(Vblend&Couette)	91% Lactose, 9% APAP, 1%MgSt	1947	2%, 5%, 8%	10	0.5269	13.213	4.513	1.599	0.579	0.216	0.103	0.583
22	12	Blend 1280 rev(Vblend&Couette)	91% Lactose, 9% APAP, 1%MgSt	2147	2%, 5%, 8%	10	0.66	14.34	4.845	1.714	0.62	0.223	0.115	0.623
23	13	Blend(Vblend)	99%lactose,1%MgSt	1698	2%, 5%, 8%, 20%, 50%, 80%	10	0.3857	7.522	2.436	0.794	0.262	0.08	0.05	0.365
24	14	Blend(Vblend)	99%lactose,1%MgSt	1698	2%, 5%, 8%, 20%, 50%, 80%	10	0.3857	7.522	2.436	0.794	0.262	0.08	0.05	0.365
25	15	Blend(Vblend&Couette)	99%lactose,1%MgSt	2077	2%, 5%, 8%, 20%, 50%, 80%	10	0.2724	6.639	2.178	0.761	0.281	0.119	0.114	0.379
26	16	Blend(Vblend&Couette)	99%lactose,1%MgSt	2077	2%, 5%, 8%, 20%, 50%, 80%	10	0.2724	6.639	2.178	0.761	0.281	0.119	0.114	0.379

4.1 Chromatography profiles

From section 2 we can see that the retention time is the basis of surface energy calculations. Since the retention time is obtained from the chromatograms, the analysis of chromatograms plays an important role in surface energy measurement. In this section we will investigate the repeatability of the chromatograms considered in this study, as indication of the repeatability of the experimental method.

4.1.1 Repeatability within a column

We repeated pure lactose 43-53μm (column 3,1948mg and column 5,1864mg), Blend (vblend & couette, column 15) for two times at the same condition. The octane curve at 2% surface coverage for each sample is presented in Fig.5. For each case, two experiments were performed and show nearly identical chromatographic peaks, which means they have the same retention time, and would provide the same surface energy calculations. Therefore, the experiments showed excellent repeatability.

4.1.2 Dependence on flow rate

The IGC provides different flow rates to measure the surface energy. In order to investigate the dependence on the flow rate we use the same column but applied two different flow rates, at 5 and 10 sccm. The flow rate directly affect the time taken for the vapor concetration front to elute down the column, which could result in different peak shapes of the chromatogram. According the Eq(4) introduced in Section2.1, the retention is expected to be inversely proportional to the flow rate. However, if the shape of the peak changes, such as if the chromatogram develops a long tail, the proportion could be broken, which

may lead to a different result of surface energy measurement for the same column with different flow rates.

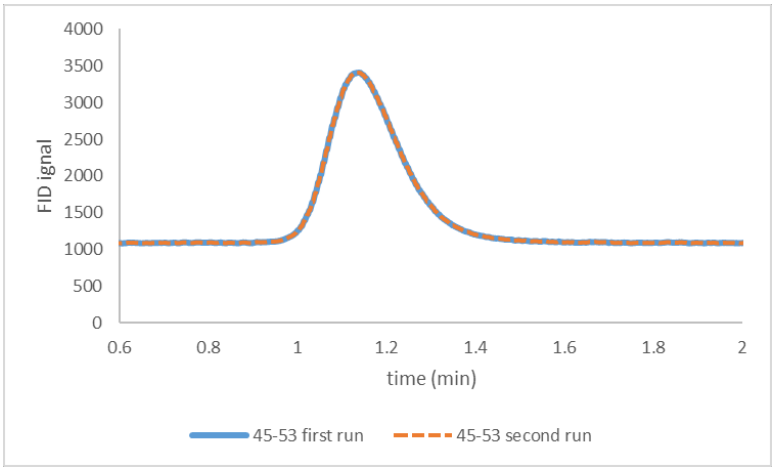

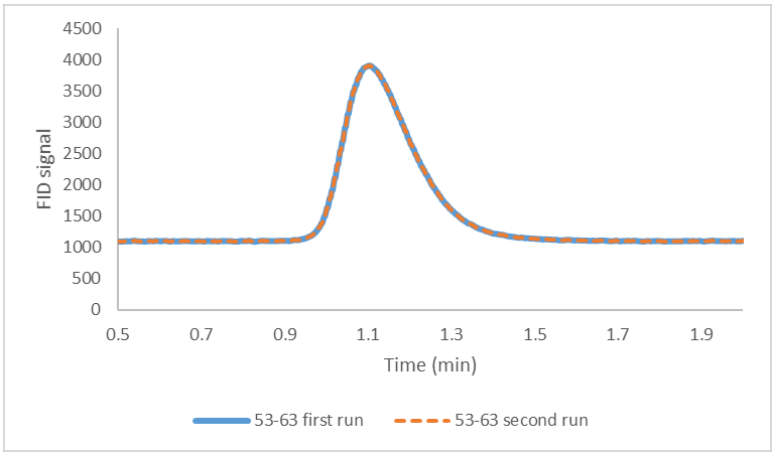

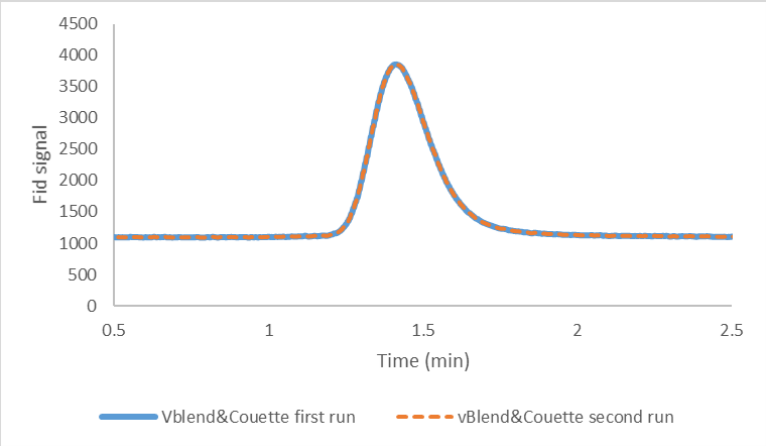

Fig.4: Octane curve at 2% surface coverage of (top) pure lactose 43-53µm (column 3,1948mg), (middle) pure lactose 43-53µm (column 5,1864mg), (bottom) Blend (vblend & couette, column 15)

Figure 4 shows 4 chromatograms of octane passing through columns at two different flow rates. It is clear that the chromatographic peak at 5 sccm has a lower peak height and a longer retention time than the chromatogram at 10 sccm. When the samples (columns) have the same material and total mass, there are only two other factors that can affect the retention volume according to the Eq (4): the net retention time and the flow rate. If we use the same column at the different flow rate, the retention volumes of the probes are expected to be the same and the retention time should therefore be inversely proportional to the flow rate.

Experiment number	**Column number**	**Component**	**Flow rate [sccm**	**Net retention time[min] (peak maximum)**	**Net retention time [min] (peak centre of mass)**
1	1	Pure lactose 38-45µm	5	2.594	2.668
2	1	Pure lactose 38-45µm	10	1.395	1.443

15	7	Pure lactose 63-75µm	5	2.034	2.098
16	7	Pure lactose 63-75µm	10	1.088	1.112

Table.2 the column information to investigate the dependence on flow rate

Since we double the flow rate, the retention time is expected to be reduced by half. By comparing the retention time ratios for experiments performed at different flow rates but in the same column, we observe that the retention times calculated based on peak maximum are closer to the expected ratios with change of flow rate, as can be observed from Table 2.

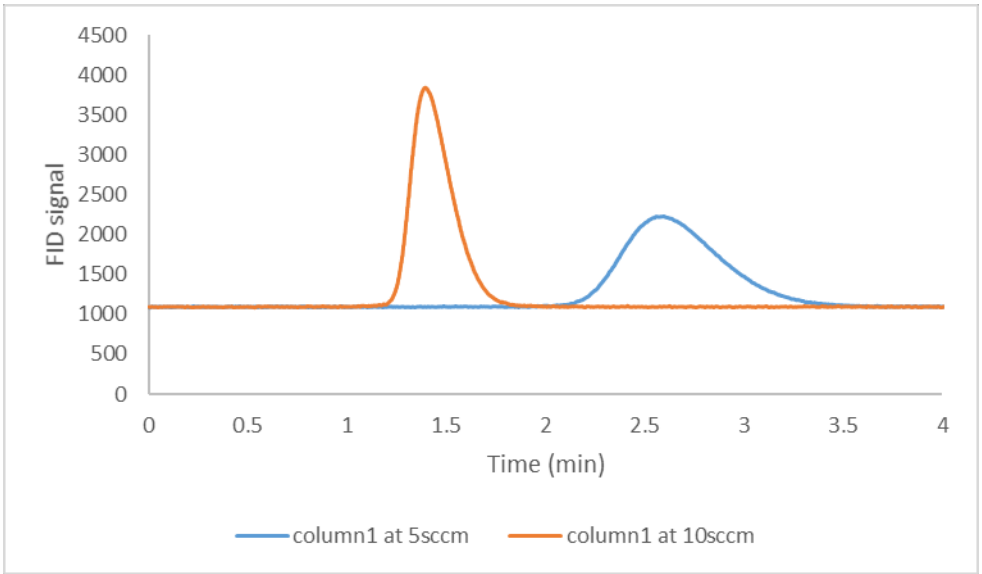

(a)

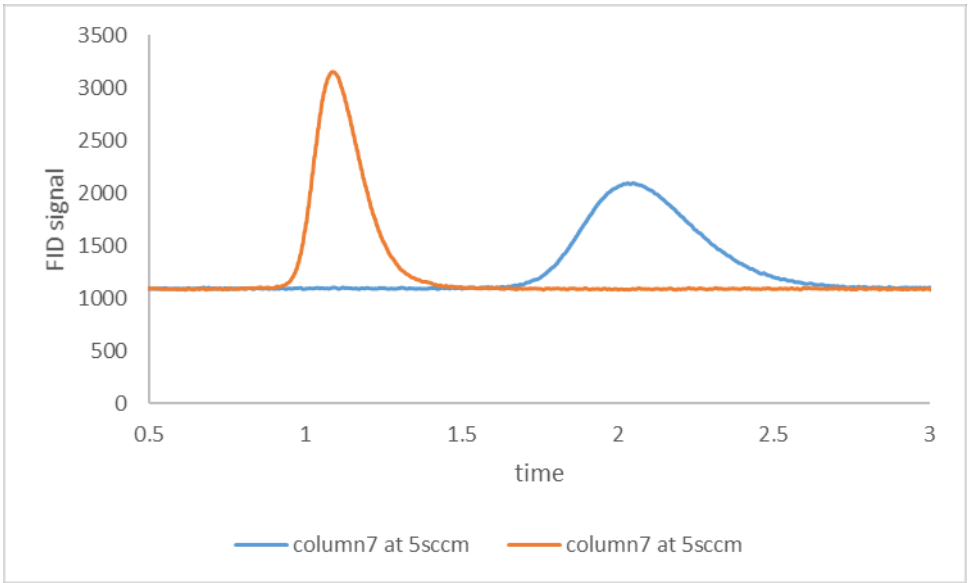

(b)

Fig.5: Octane at 0.02 surface coverage of (a) column1 at 5 and 10 sccm (b) column7 at 5 and 10sccm

4.2 BET specific surface area calculation

In this thesis, the BET surface area was calculated from octane adsorption isotherms. All experiments were carried out under the same conditions and the carrier gas flow rate was set at 10 sccm (standard cubic centimeters per minute). In all cases, the retention time was determined by the peak of center mass. The reason we selected peak centre of mass rather than peak maximum in BET measurement is because most of the elution peaks were asymmetric.

Table.3: Injections used in the BET method

Injection	solvent	Target moles injected (mMol)
1	octane	0.00006

2	octane	0.00008
3	octane	0.00010
4	octane	0.00012
5	octane	0.00015
6	octane	0.00018
7	octane	0.00020
8	octane	0.00023
9	octane	0.00028
10	octane	0.00035

First we use 10 injections of octane to set up a method for BET surface area measurement by software Cirrus SEA and used it for all the BET experiments. The amount used in the different injections is shown in Table 3. Ten injections of octane were applied to the column over a range of 0.00006 to 0.00035 mMol. Two injections of methane were both made after the first and last injection of octane, which can be used to measure the dead time and net retention time, see Fig.7. All 14 injections of column 4 are shown in Table 4. By knowing the moles of probes injected, flow rate, height of the chromatogram and chromatogram area, the partial pressure of probes can be calculated by Eq.(13). Then, the adsorbed amounts normalized by the mass of the partial pressures of adsorbed were obtained by calculating the integral of specific retention volumes over the partial pressures of the adsorbate by Eq.(14). The solvent vapor pressure was calculated with the Antoine equation [32]. The linear relationship of the BET Eq. (15) can be obtained by plotting $1/n(P_0/P) - 1]$ versus P_0/P. Since the R^2 should be bigger than 0.995 and the linear relationship of the BET equation is only maintained in the range of between 0.05 and 0.35,

some points need to be excluded, in this case the first two points have been excluded since they are outside the linear regime. Figure 6 shows the BET plot corresponding to column 4. The BET constant c in Eq. 15 and the monolayer capacity can be calculated from the slope and intercept of the line, which in this case are 3.2185 and 0.3100 mMol/g [33]. The surface area then can be determined by the Eq. (16), which in this case is 0.3100 m^2/g. Results obtained for other columns are listed in Table 4.

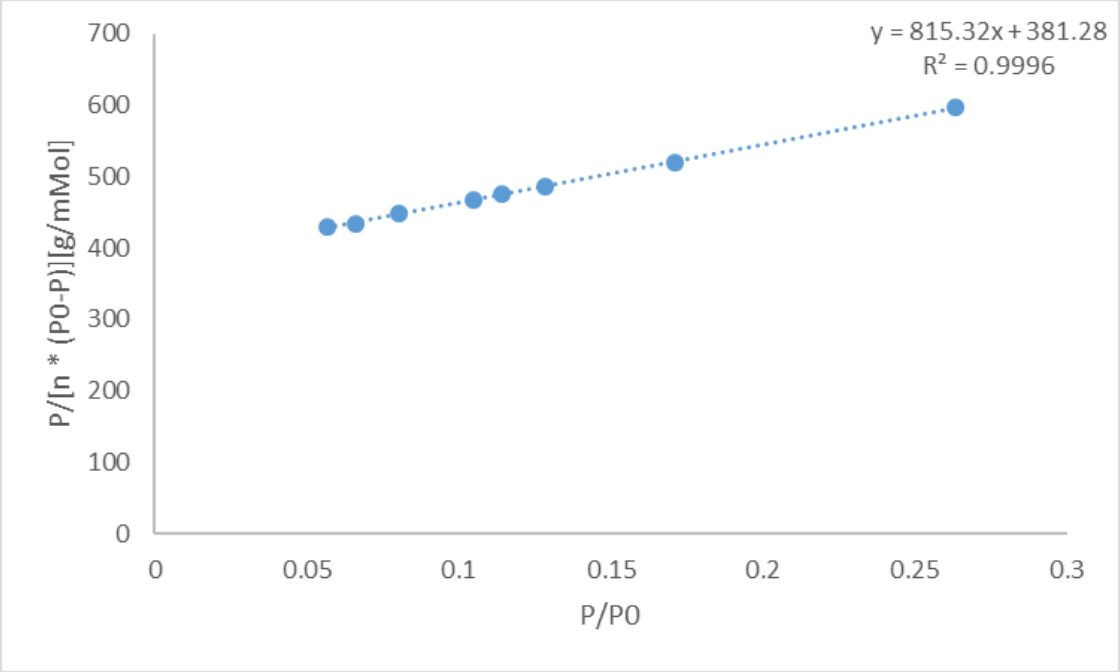

Fig.6: The plot of BET octane method for lactose at 53-63m (column 4 in the Table 1)

Table.4: BET method data for Exp.10

Injection Name	Target moles Injected [10^{-5}·mMol]	Injected Amount [10^{-5}·mMol]	Partial Pressure [Torr]	Absorbed Amount [10^{-5}·mMol]	H_{peak} [µV]	Peak Area [µV·min]
Methane1					85300	10828
Methane2					85323	10834
Octane1	6	5.39	0.4395	7.97	5237	1093

Octane2	8	7.67	0.6169	11.1	7583	1600
Octane3	10	9.86	0.7948	14.0	9919	2096
Octane4	12	11.4	0.9247	16.2	11667	2452
Octane5	15	13.7	1.1266	19.5	14404	2973
Octane6	18	18.5	1.6041	27.0	20985	4127
Octane7	20	17.3	1.4719	25.0	19141	3831
Octane8	23	20.5	18043	30.2	23781	4595
Octane9	28	25.9	2.4019	39.6	32222	5919
Octane10	35	38.2	3.6919	59.2	50984	8990
Methane3					85226	10801
Methane4					84352	10680

4.3 Surface Energy calculation

The surface energy calculation is based on the net retention time of the probes. All the experiments follow the same calculation steps, and we shall use lactose 53-63mm (Experiment10) as an example. First, the net retention time can be obtained by subtracting the dead time from the retention time, see Fig.7. The net retention time of lactose 53-63mm (Exp.10) is shown in Table.5. Then, the specific retention time can be obtained from Eq.4. As we mentioned in the previous section, the dispersive surface energy can be obtained from a plot of $RTlnV_N$ versus $N_A a_m$, see Fig.8. The dispersive energy of the solid is calculated from the slope of the linear regression. The difference between the alkane line and the polar probe equates to ΔG_{ab}^0 acid-base adsorption component of the Gibbs free energy. In Van Oss description the specific component of surface free energy can be divided into the contribution of electron acceptor and electron donor, which can be calculated by Eq.11. The results of surface energy for lactose 53-63mm (Exp.10) is listed in Table.6.

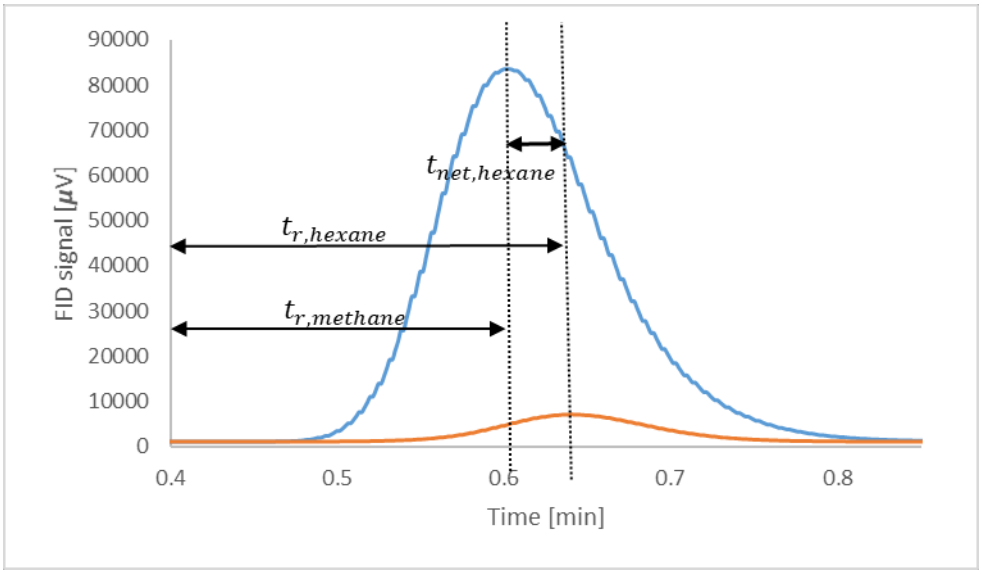

Fig. 7: The net retention time of Hexane in lactose 53-63mm (Exp.10)

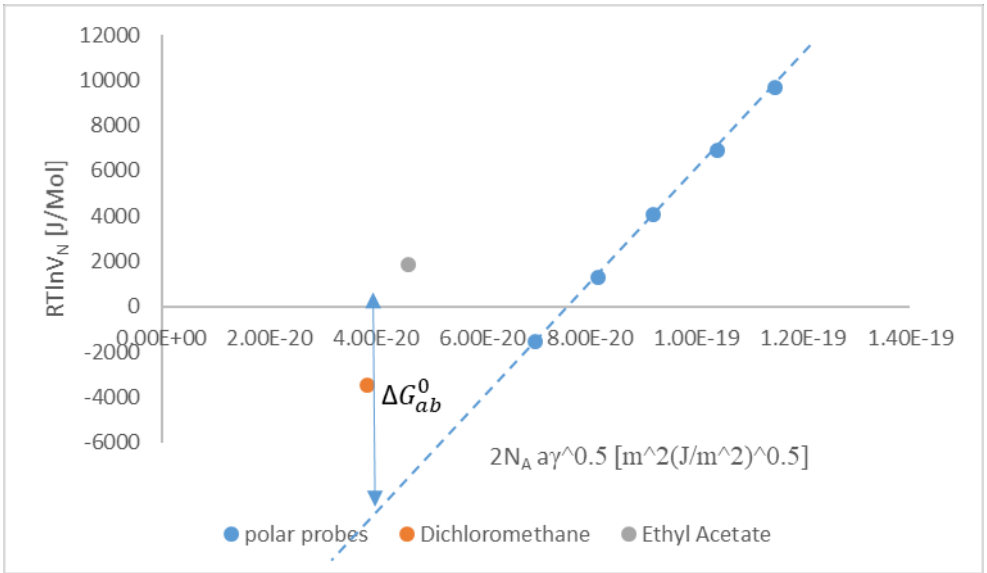

Fig.8: Determination of solid-vapor surface free energy and acid/base free energy change of adsorption from Schultz approach

Table.5: The net retention time of each probe for Exp.10.

Injection Solvent	Surface Coverage	Net Retention Time [min]
Decane	0.02	5.264
Decane	0.05	4.555
Decane	0.08	4.281
Nonane	0.02	1.789

Nonane	0.05	1.582
Nonane	0.08	1.491
Octane	0.02	0.616
Octane	0.05	0.541
Octane	0.08	0.518
Heptane	0.02	0.205
Heptane	0.05	0.183
Heptane	0.08	0.181
Hexane	0.02	0.065
Hexane	0.05	0.058
Hexane	0.08	0.056
Dichloromethane	0.02	0.030
Dichloromethane	0.05	0.020
Dichloromethane	0.08	0.023
Ethyl Acetate	0.02	0.218
Ethyl Acetate	0.05	0.156
Ethyl Acetate	0.08	0.131

Table.6: The surface energy of Experiment10

Surface coverage	**γd [mJ/m^2]**	**γab [mJ/m^2]**	**γt [mJ/m^2]**
0.02	40.3509756	85.7938203	126.144796
0.05	39.9647371	70.3895604	110.354297
0.08	39.3471292	68.6827578	108.029887

5. Case studies

By using the results from section 4 we are able to investigate changes in surface energy of pharmaceutical powders depending on particle size of the powder and on the magnitude of shear strain applied to a pharmaceutical blend.

5.1 Lactose with different particle sizes

In section 4.3, the detailed procedure to obtain the surface energy of a powder sample by measuring the retention time of several vapors passing through the sample is described. This method is used in this section to calculate the surface energy of powder samples of different particle sizes from 38 to 106 microns, obtained from the same lot of commercially available lactose as explained in section 3. The sample of about 2000mg of each particle size is inserted into the IGC column as described in section 3 and its surface area is measured by the procedure described in section 4.2(BET). In order to investigate the correlation between the particle size and specific surface area. We first calculate the average particle size (R) of each material. Then we plot specific surface area versus 1/R. As can be shown in figure Fig.9, the specific surface area goes as the inverse of particle size. The point of 45-53μm has been excluded since it seems to be something weird with that point and it doesn't follow the trend.

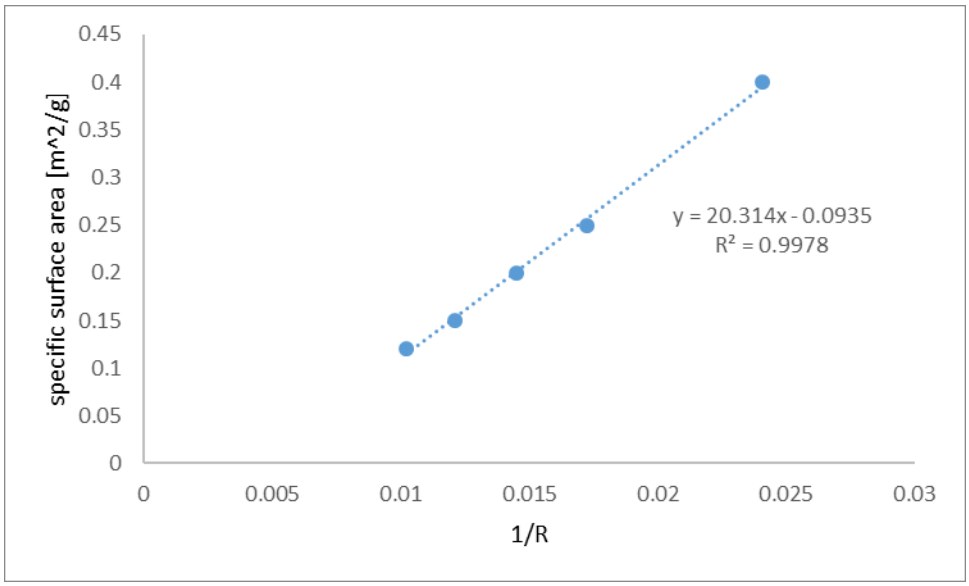

Fig.9 specific surface area per unit mass as the function of the particle size

The surface energy is obtained for different coverages by using the 7 vapors as described in section 4.3. The dispersive energy of lactose with different particle size fell into the range of 37 mJ/m^2 to 47 mJ/m^2, which is in good agreement with values reported in the literature (Newell et al., 2001). Both the dispersive and the polar energies of all the samples decrease with increasing surface coverage as shown in the graphs of Fig.10 (a) and (b) respectively. This trend is reasonable and has been seen in most materials [34, 35] and it is attributed to the fact that at low surface coverages, the high energy sites are first taken up by the probe molecules; increasing the surface coverage leads to the occupation of lower energy sites by the probe, lowering the energy measured at larger surface coverage. The polar surface energy does not show a definitive trend with particle size, especially at the lowest coverage of 0.02. Because the dispersive energy of each sample is similar, the distribution of the total surface energy of all the samples is similar to the distribution of the polar surface energy.

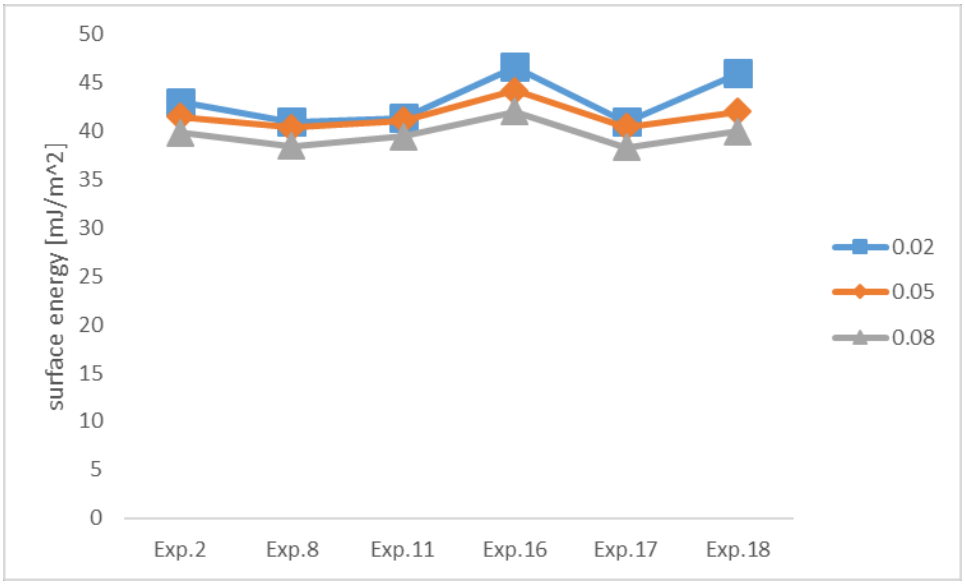
50
45
40
35
30
25
20
15
10
5
0
surface energy [mJ/m^2]
Exp.2
Exp.8
Exp.11
Exp.16
Exp.17
Exp.18
0.02
0.05
0.08

(a)

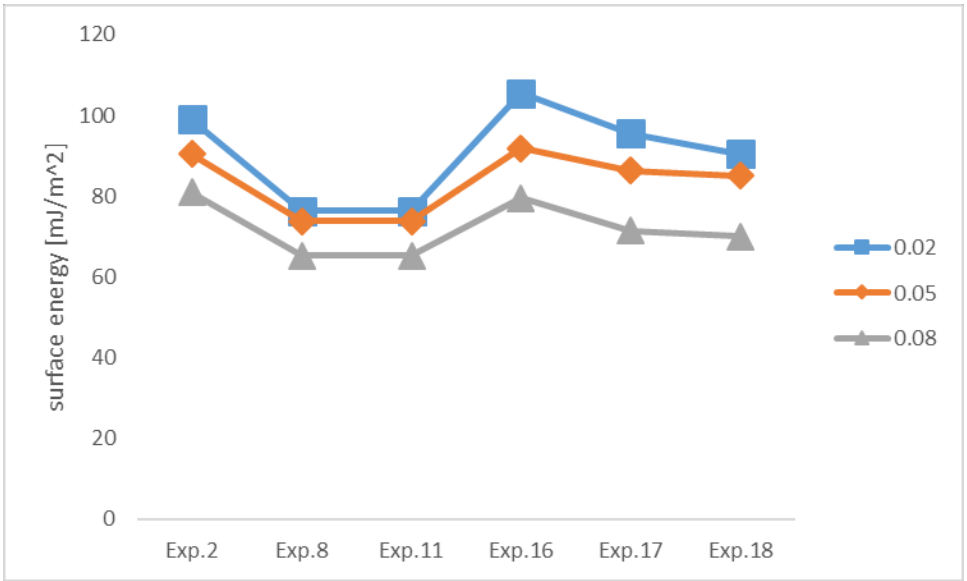
120
100
80
60
40
20
0
surface energy [mJ/m^2]
Exp.2
Exp.8
Exp.11
Exp.16
Exp.17
Exp.18
0.02
0.05
0.08

(b)

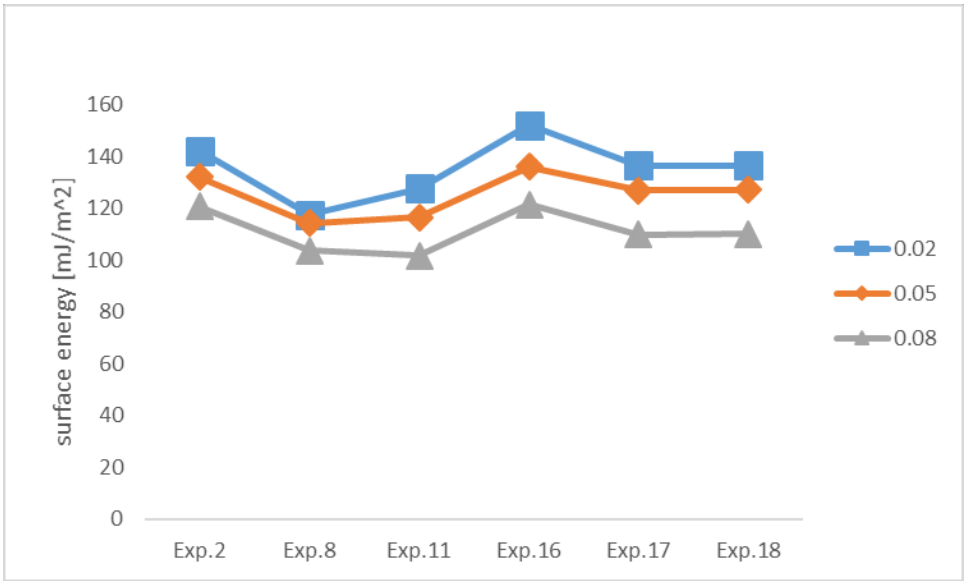

(c)

Fig.9: Surface energy of different particle size (a) dispersive energy (b) specific surface energy (c)total surface energy

5.2 Lactose-MgSt Blends

The surface energy for Lactose- MgSt blends (processed as described in section 3.2) are displayed in Fig.10. The dispersive energies of lactose with V-blend processing at surface coverage 0.02, 0.05, 0.08 fell into the range between 40 mg/m^2 to 44mJ/m^2, which is similar to the pure lactose. The surface energy decreases with the surface coverage increase again as expected. The values for dispersive energy at surface coverages 0.02, 0.05, 0.08 of the blends where extra sheer stress has been applied with the Couette equipment are in the range from 35mJ/m^2 to 36mJ/m^2. This is approximately 25% lower than the dispersive energy of lactose and the blends without Couette processing. This effect can be explained by the fact that the magnesium stearate (a shear sensitive material) dry coats the surface of the lactose particles as more shear is imparted to the blend.

Magnesium stearate is a lubricant that is known to be hydrophobic [36] with a low surface energy[12].

At higher surface coverages than 20%, the dispersive surface energy of the blends that were processed in the shearing device show an uncommon increasing trend. Like we mentioned in the previous section, the chromatographic peaks under finite dilution can show either “tailing” or “fronting” shape. In the ‘tailing” situation, the adsorption isotherm is characterized by a Type I, II, or IV with the formation of a monolayer of adsorbate on the adsorbent. However, in our experiments, the chromatograms are like in Fig 11. As will be discussed in the section 6.1, this means that there is a variation of the local solute velocity with solute concentration, in the present case, this variation is “overloading” in type.

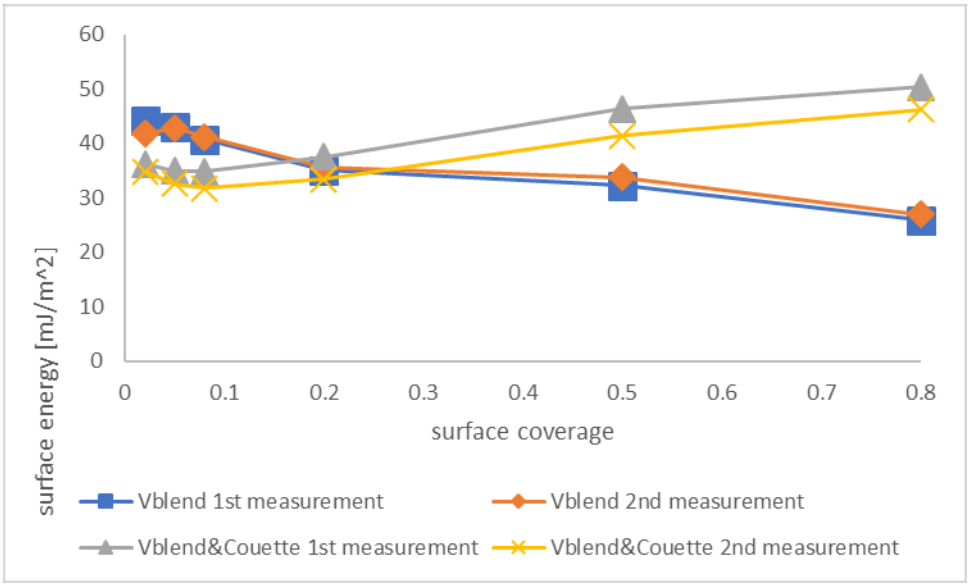

(a)

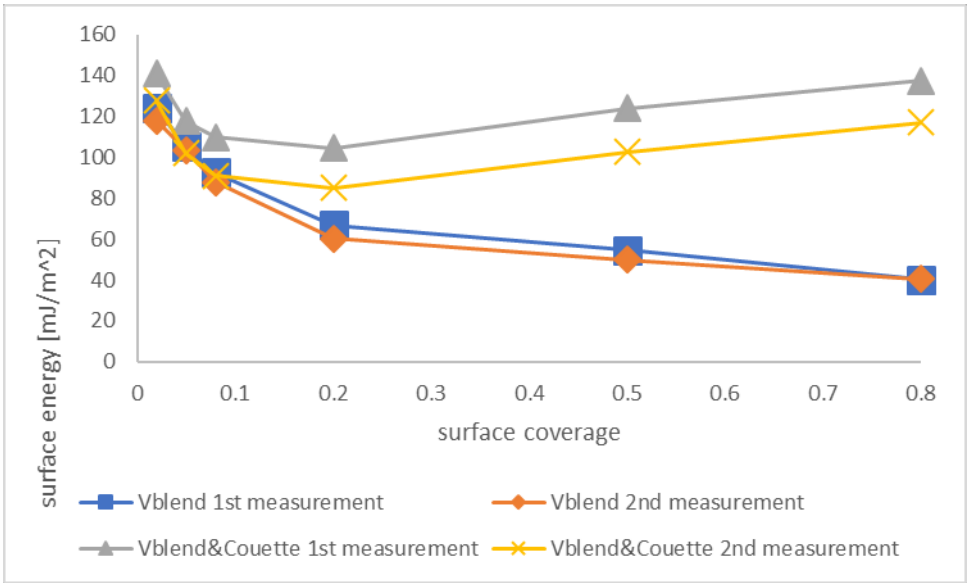

(b)

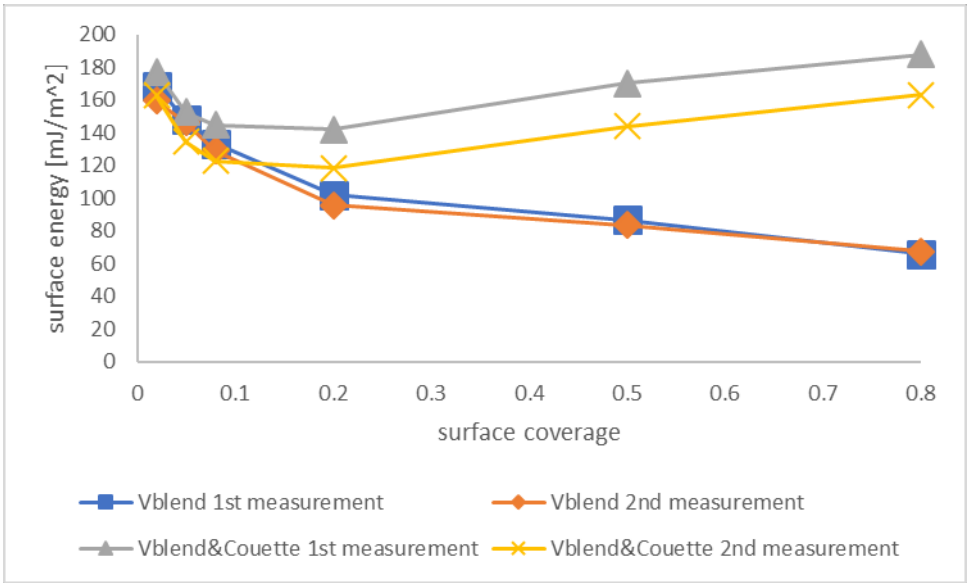

(c)

Fig.10: Surface energy of blends with different processing (a) dispersive energy (b) specific surface energy (c) total surface energy

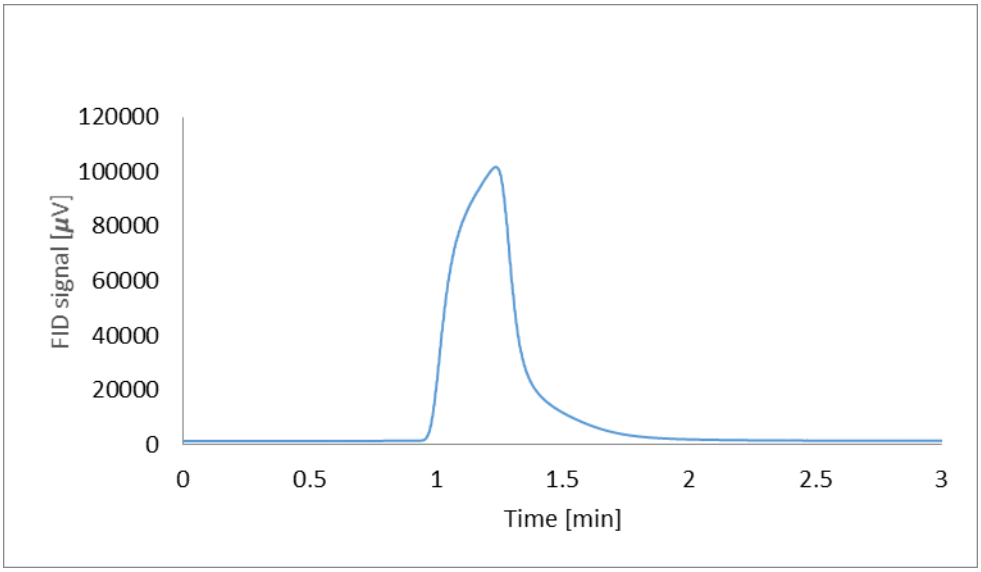

Fig.11: the octane chromatogram at 80% surface coverage of Exp.11

6. Some problems found

This chapter is devoted to showing some of the problems that were found when using IGC method to determine surface energy of powders to report their existence and to promote future studies in the subject.

6.1 Asymmetric peak

It can be observed that the shape of the peaks does not follow the law of ideal chromatography which is that the peaks should have a gaussian shape and be symmetric. There might be two reasons why this is not the case: (1) As the hydrocarbon chain length increases the interaction between the probes and sample surface also increases. This results in a longer retention time of longer molecules with respect to smaller ones. The increased residence time in the GC column for the

larger molecule mass alkanes directly results in border and less intense solute peaks due to increased longitudinal diffusive broadening. The peaks then don't maintain the Gaussian shape. (2) At high concentration, the surface sites become almost saturated with mobile phase and will adsorb very little. For this reason, the mobile phase vapor fraction increases with vapor concentration. Thus, the vapor migrates fastest at the center of the zone where the overall concentration is greatest. The center of the zone consequently overtakes the leading edge while leaving the trailing edge behind, the zone profile loses its symmetry and forms a sharp rapidly moving front and a gradually descending rear.

6.2 The use of dichloromethane

To apply the van vOCG approach to obtain the acid and basic components of the polar surface energy of the solid materials, monopolar probes are necessary to pass through the column. The only acid monopolar probe that can be seen in literature is dicholoromethane. However, this probe has an important problem: the retention volume is usually very close to zero, or the total time to pass through the system is very similar to the time for methane (used as the reference of a non retaining vapor) as can be seen in the examples shown in Fig.8. This particular fact poses a great uncertainty in the calculation of the acid component of the solid surface energy. This is the reason for the large variation in the polar surface energy in general, but to our knowledge, it has not been reported before in literature and SSM, the company selling the instrument, is still recommending this vapor to do the analysis.

To highlight the above mentioned fact, we can add that due to inherent variability of the process, in some cases the retention time obtained for dichloromethane at lower surface coverage was smaller than for methane. One possibility to increase the resolution of the determination of the dichloromethane retention volume is to decrease the flow rate of the carrier gas. The problem with

that is that high alkanes like decane (and possibly nonane) may not be suitable to be used to obtain the dispersive component at very low flow rate due to extensive chromatogram deformation.

6.3 Surface coverage limitation

In our experiments, we excluded decane for all measurements of blends. This is because that in IGC measurements, the probe with lager molecule mass such as decane sometimes can only be applied in a small range of surface coverage. The reason might be that the IGC experiments at 25℃ is not able to provide enough decane vapor to cover the target surface coverage. Since the decane cannot be used, only four alkanes are used to calculate the dispersive component of the surface energy of the material, which may affect the accuracy of the result.

7. Conclusions

In our study the surface energy of pure lactose with different particle size and blends with two different processing was measured using IGC, which is also the first thesis on IGC in the group. Overall, the surface energy of lactose with different particle size has no specific trending. And there is a measurable reduction in the dispersive energy of lactose-MgSt. The reduction in the dispersive energy of lactose with lubrication was attributed to coverage of some of the high energy sites on the lactose by MgSt. The reason that the surface energy of blends applied with Couette processing goes up with increasing surface coverage is because that after applying shears to the Lactose-MgSt blends, the MgSt can be more spread. When the MgSt is spread in the powder, the

multilayers start happening at high surface coverage. Since the multilayers occurs, it takes a longer time for mobile phase to pass through the stationary phase. Then the surface energy increases with the increasing of the retention volume.

References

1. Wenzel, T., *Separation Science - Chromatography Unit.* From www.chem.libretext.org at https://chem.libretexts.org/Bookshelves/Analytical_Chemistry/Supplemental_Modules_(Analytical_Chemistry)/Analytical_Sciences_Digital_Library/Active_Learning/In_Class_Activities/Separation_Science, 2019.
2. Grimsy, I.M., et al, *analysis of teh surface energy of pharmaceutical powders by inverse gas chromatography.* Journal of pharmaceutical science, 2001. **91**: p. 571-583.
3. Smith, R.R., et al., *A new method to determine dispersive surface energy site distributions by inverse gas chromatography.* Langmuir, 2014. **30**(27): p. 8029-35.
4. R.Williams, D., *Particle Engineering in Pharmaceutical Solids Processing: Surface Energy Considerations.* Current Pharmaceutical Design, 2015.
5. Jones, M.D., P. Young, and D. Traini, *The use of inverse gas chromatography for the study of lactose and pharmaceutical materials used in dry powder inhalers.* Adv Drug Deliv Rev, 2012. **64**(3): p. 285-93.
6. Mohammadi-Jam, S. and K.E. Waters, *Inverse gas chromatography applications: a review.* Adv Colloid Interface Sci, 2014. **212**: p. 21-44.
7. Das, S.C., et al., *Determination of the polar and total surface energy distributions of particulates by inverse gas chromatography.* Langmuir, 2011. **27**(2): p. 521-3.
8. Karde, V. and C. Ghoroi, *Influence of surface modification on wettability and surface energy characteristics of pharmaceutical excipient powders.* Int J Pharm, 2014. **475**(1-2): p. 351-63.
9. Ho, R. and J.Y.Y. heng, *A review of inverse gas chromatographhyh and its development as a tool characterize anisotropic surface properties of pharmaceutical solids.* KONA powder and particle journal No.30 2012.
10. Rosenberg, R.M. and W.L. Peticolas, *Henry's Law: A Retrospective.* Journal of Chemical Education, 2004. **81**(11): p. 1647.
11. Thielmann, F., *Introduction into the characterisation of porous materials by inverse gas chromatography.* Journal of Chromatography A, 2004. **1037**(1-2): p. 115-123.
12. Schultz J, L.L., Martin C., *Schultz J, Lavielle L, Martin C. The role of the interface in carbon fibre-epoxy composites.* J Adhes, 1987.
13. Dorris, G.M. and D.G. Gray, *Adsorption of n-alkanes at zero surface coverage on cellulose paper and wood fibers.* Journal of Colloid and Interface Science, 1980. **77**(2): p. 353-362.
14. Schultz J, L.L., *Interfacial properties of carbon fiber-epoxy matrix composites. Inverse gas chromatography characterisation of polymers and other materials.* ACS Symposium Ser, 1989. **391**.

15. Newell HE, B.G., Butler DA, Thielmann F, Williams DR. , *The use of inverse phase gas chromatography to measure the surface energy of crystalline, amorphous, and recently milled lactose.* . Pharm Res, 2001. **18**.
16. Ho R, H.J., *A review of inverse gas chromatography and its development as a tool to characterize anisotropic surface properties of pharmaceutical solids.* KONA Powder Part J, 2013.
17. Voelkel, A., *Inverse gas chromatography as shource of physicochemical data.* Journal of Chromatography A, 2009. **1216**.
18. Balard H, B.E., Papirer E. Determination of the acid–base properties of solid, *Determination of the acid–base properties of solid surfaces using inverse gas chromatography: advantages and limitations.* . Acid–Base Interactions, Relevance to Adhesion Science and Technology., 2000. **2**.
19. Voelkel, A., *Chapter 2.5 Inverse gas chromatography in the examination of acid-base and some other properties of solid materials*, in *Studies in Surface Science and Catalysis*, A. Dąbrowski and V.A. Tertykh, Editors. 1996, Elsevier. p. 465-477.
20. Fowkes, F.M., *Attractive forces at interfaces.* . Ind Eng Chem 1964. **56**.
21. Wang, W., et al., *Surface properties of solid materials measured by modified inverse gas chromatography.* Talanta, 2013. **112**: p. 69-72.
22. Ylä-Mäihäniemi PP, H.J., Thielmann F, Williams DR.. *Inverse gas chromatographicmethod for measuring the dispersive surface energy distribution for particulates.* Langmuir, 2008. **25**.
23. Mel'gunov, M.S. and A.B. Ayupov, *Direct method for evaluation of BET adsorbed monolayer capacity.* Microporous and Mesoporous Materials, 2017. **243**: p. 147-153.
24. *S. Brunauer, P.H. Emmett, E. Teller, J. Am. Chem. Soc. 60 (1938) 309e319.*
25. *J. Rouquerol, F. Rouquerol, P. Llewellyn, G. Maurin, K.S.W. Sing, Adsorption by Powders and Porous Solids: Principles, Methodology and Applications, second ed., Academic Press, 2014.*
26. *F. Thielmann, Introduction into the characterisation of porous materials by inverse gas chromatography, J. Chromatogr. A 1037 (12) (2004) 115–123.*
27. Legras, A., et al., *Inverse gas chromatography for natural fibre characterisation: Identification of the critical parameters to determine the Brunauer-Emmett-Teller specific surface area.* J Chromatogr A, 2015. **1425**: p. 273-9.
28. *B. Charmas, R. Leboda, Effect of surface heterogeneity on adsorption on solid surfaces: application of inverse gas chromatography in the studies of energetic heterogeneity of adsorbents, J. Chromatogr. A 886 (12) (2000) 133–152.*
29. *Thommes, M. (2016). Physisorption of gases, with special reference to the evaluation of surface area and pore size distribution (IUPAC Technical Report). Chemistry International, 38(1), pp. 25-25. Retrieved 18 Mar. 2019, from doi:10.1515/ci-2016-0119.*
30. Raghavan, S.R., Radoljub B Sheen, D Sherwood, *Dissolution Kinetics of Single Crystals of α-Lactose Monohydrate.* J. Pharm. Sci, 2002(10): p. 2166.
31. Mehrotra Amit, L.M., Faqih Abdul, Levin, Michael, Muzzio, Fernando J., *Influence of shear intensity and total shear on properties of blends and tablets of lactose and cellulose lubricated with magnesium stearate.* International Journal of Pharmaceutics, 2007. **336**(2): p. 284-291.
32. *R.H. Perry, D.W. Green, J.O. Maloney, Perry's Chemical Engineers Handbook, McGraw Hill, New York, 1997.*

33. Jong, T., et al., *Investigation of the Changes in Aerosolization Behavior Between the Jet-Milled and Spray-Dried Colistin Powders Through Surface Energy Characterization.* Journal of Pharmaceutical Sciences, 2016. **105**(3): p. 1156-1163.
34. Das, S.C., et al., *Use of surface energy distributions by inverse gas chromatography to understand mechanofusion processing and functionality of lactose coated with magnesium stearate.* Eur J Pharm Sci, 2011. **43**(4): p. 325-33.
35. Lapčík, L., et al., *Surface heterogeneity: Information from inverse gas chromatography and application to model pharmaceutical substances.* Current Opinion in Colloid & Interface Science, 2016. **24**: p. 64-71.
36. Zhanjie Liu, Y.W., Fernando J. Muzzio, Gerardo Callegari, German Drazer, *Capillary drop pentration method to characterize the liquid wetting of powders.* Langmuir, 2017.